Cerebral Cortex June 2014;24:1422–1435
doi:10.1093/cercor/bhs410
Advance Access publication January 11, 2013

# Impaired Long Distance Functional Connectivity and Weighted Network Architecture in Alzheimer's Disease

Yong Liu[1,2], Chunshui Yu[3], Xinqing Zhang[4], Jieqiong Liu[4], Yunyun Duan[5], Aaron F. Alexander-Bloch[2], Bing Liu[1], Tianzi Jiang[1,6,7] and Ed Bullmore[2,8]

[1]LIAMA Center for Computational Medicine, National Laboratory of Pattern Recognition, Institute of Automation, The Chinese Academy of Sciences, Beijing 100190, China [2]Brain Mapping Unit, Department of Psychiatry, University of Cambridge, Cambridge CB2 3EB, UK [3]Department of Radiology, Tianjin Medical University General Hospital, Tianjin 300052, China [4]Department of Neurology, [5]Department of Radiology, Xuanwu Hospital of Capital Medical University, Beijing 100053, China [6]Key Laboratory for NeuroInformation of Ministry of Education, School of Life Science and Technology, University of Electronic Science and Technology of China, Chengdu 610054, China [7]The Queensland Brain Institute, The University of Queensland, Brisbane QLD 4072, Australia and [8]Clinical Unit Cambridge, GlaxoSmithKline, Addenbrooke's Hospital, Cambridge CB2 0SZ, UK

Address correspondence to Tianzi Jiang, LIAMA Center for Computational Medicine, National Laboratory of Pattern Recognition, Institute of Automation, Chinese Academy of Sciences, Beijing 100190 China. Email: jiangtz@nlpr.ia.ac.cn; Y. L., C. Y., and X. Z. have made equal contributions to this work and should be regarded as joint first authors.

**Alzheimer's disease (AD) is increasingly recognized as a disconnection syndrome, which leads to cognitive impairment due to the disruption of functional activity across large networks or systems of interconnected brain regions. We explored abnormal functional magnetic resonance imaging (fMRI) resting-state dynamics, functional connectivity, and weighted functional networks, in a sample of patients with severe AD (*N* = 18) and age-matched healthy volunteers (*N* = 21). We found that patients had reduced amplitude and regional homogeneity of low-frequency fMRI oscillations, and reduced the strength of functional connectivity, in several regions previously described as components of the default mode network, for example, medial posterior parietal cortex and dorsal medial prefrontal cortex. In patients with severe AD, functional connectivity was particularly attenuated between regions that were separated by a greater physical distance; and loss of long distance connectivity was associated with less efficient global and nodal network topology. This profile of functional abnormality in severe AD was consistent with the results of a comparable analysis of data on 2 additional groups of patients with mild AD (*N* = 17) and amnestic mild cognitive impairment (MCI; *N* = 18). A greater degree of cognitive impairment, measured by the mini-mental state examination across all patient groups, was correlated with greater attenuation of functional connectivity, particularly over long connection distances, for example, between anterior and posterior components of the default mode network, and greater reduction of global and nodal network efficiency. These results indicate that neurodegenerative disruption of fMRI oscillations and connectivity in AD affects long-distance connections to hub nodes, with the consequent loss of network efficiency. This profile was evident also to a lesser degree in the patients with less severe cognitive impairment, indicating that the potential of resting-state fMRI measures as biomarkers or predictors of disease progression in AD.**

**Keywords:** Alzheimer's disease, disconnection, distance, functional connectivity, weighted brain networks

## Introduction

The human brain is organized into parallel, segregated complex systems with different functional areas that are specialized for processing distinct forms of information (Tononi et al. 1998; Sporns 2010, 2011). Information exchange between interconnected brain regions is believed to be the biological basis for human cognitive processes (Horwitz 2003). Indeed, the human brain is an effective functional system, which reaches a balance between local specialization and global integration. Understanding the complex local and global brain activity patterns can offer new insights into general organizational principles of brain function (Sporns and Zwi 2004; Sporns 2010).

Alzheimer's disease (AD) is one of the most common neurodegenerative diseases to endanger human health in the world. Clinically, AD is characterized by early stage memory impairment, and by more extensive cognitive impairments in later stages. On the other hand, mild cognitive impairment (MCI) represents an intermediate state of cognitive function between changes seen in normal aging and those fulfilling the criteria for AD (Petersen et al. 1999; Petersen 2009). Previous studies demonstrated that MCI, especially amnestic MCI, will convert to AD at about 10–15% annual rate (Rami et al. 2007; Petersen 2009; Landau et al. 2010; Pozueta et al. 2011), or even 20% per year (Fischer et al. 2007; Maioli et al. 2007). This means that roughly 30–50% of MCI subjects will convert to AD within 3–5 years.

Previous studies suggest that AD is not only associated with regional damage, but also with abnormal functional integration of different brain regions through disconnection mechanisms (Delbeuck et al. 2003, 2007; Bozzali et al. 2011). Previous functional magnetic resonance imaging (fMRI) studies found alterations of activation patterns in both MCI and AD patients during cognitive tasks (Lustig et al. 2003; Pariente et al. 2005; Rombouts, Barkhof, et al. 2005; Rombouts, Goekoop, et al. 2005; Celone et al. 2006; Buckner et al. 2008; Bajo et al. 2010) and at resting-state (Li et al. 2002; Greicius et al. 2004; Wang et al. 2006; Allen et al. 2007; He et al. 2007; Wang et al. 2007; Bai et al. 2009; Wang, Yan, et al. 2011; Zhang et al. 2012). Furthermore, local and global functional connectivity disruptions in AD/MCI have been found using graph analysis on fMRI (Wang et al. 2007; Supekar et al. 2008; Sanz-Arigita et al. 2010; Wang, Zuo, et al. 2012; Zhao et al. 2012), diffusion MRI (Lo et al. 2010), electroencephalography (EEG; Stam et al. 2007), magnetoencephalography (MEG; Stam et al. 2009; Buldu et al. 2011), and structural MRI data (He et al. 2008; Yao et al. 2010). These and other data have

supported the idea that AD is a disconnection syndrome (Delbeuck et al. 2003, 2007; Bozzali et al. 2011).

In this study, we directly investigated the hypothesis that the brain network of AD is characterized by functional disruption both in local univariate time series statistics as well as bivariate and global measures of functional connectivity and functional network organization. We predicted that patients with severe AD would demonstrate abnormalities of brain function especially in highly connected hub regions of the cortex, including components of the default mode network, such as medial posterior parietal cortex and dorsal medial prefrontal cortex. We also expected that brain functional abnormalities present to a higher degree in patients with severe AD would be evident also to a lesser degree in patients with less severe AD and MCI; and that resting-state fMRI markers of abnormal brain function would be correlated with variation between patients in the severity of cognitive impairment as measured by the mini-mental state examination (MMSE). To test these hypotheses, we measured local oscillatory dynamics and low-frequency correlations between 442 cerebral regions in fMRI data acquired under no-task conditions from 18 patients with severe AD, 17 patients with mild AD, 18 patients with MCI, and 21 age-matched healthy volunteers. We constructed graphical models of brain networks and estimated weighted topological properties to explore the impact of AD on long-distance connections mediating efficient network information transfer (Fig. 1). In addition to these case–control comparisons between patients with AD and healthy volunteers, we also explored correlations between MMSE scores and brain functional markers estimated over all patients.

## Materials and Methods

### *Subjects*

All the participants were recruited by advertisement and supported throughout the testing procedures in a specialist neuropsychological research facility at Xuanwu Hospital, Beijing, China. Patients and informants (usually a family member) were clinically interviewed by a senior neurologist (X.Z.). Written consent forms were obtained from all subjects or their legal guardians (usually a family member). The study was approved by the ethics committee of Xuanwu Hospital. AD subjects were diagnosed using standard operationalized criteria (Diagnostic and Statistical Manual of Mental Disorders, Fourth Edition(DSM-IV); American Psychiatric Association 1994 and National Institute of Neurological and Communicative Disorders and Stroke - Alzheimer's Disease and Related Disorders Association (NINCDS-ADRDA); McKhann et al. 1984). The severity of dementia was assessed using the Clinical Dementia Rating (CDR) scale (Morris 1993). Patients with a diagnosis of AD and CDR score of 1 were classified as mild AD and those with a CDR score of 2 or 3 were diagnosed as severe AD. MCI was diagnosed according to standard criteria (Petersen et al. 1999, 2001; Choo et al. 2007), which included subjective memory loss with objective evidence of memory impairment in the context of normal or near-normal performance on other domains of cognitive functioning; minimal impairment of activities of daily living; and a CDR score of 0.5. Normal volunteers have a CDR score of 0.

All participants satisfied the following inclusion criteria: 1) no history of an affective disorder within 1 month prior to assessment; 2) normal vision and audition; 3) able to cooperate with cognitive testing; 4) aged between 50 and 90 years; 5) no clinical history of stroke or other severe cerebrovascular disease; and 6) no more than one lacunar infarction, without patchy or diffuse leukoaraiosis, on neuroradiological assessment of conventional MR images.

The exclusion criteria included: 1) severe general medical disorders of cardiovascular, endocrine, renal, or hepatic systems; neurological disorders associated with potential cognitive dysfunction, including local brain lesions, traumatic brain injury with loss of consciousness or confusion, and dementia associated with neurosyphilis, Parkinsonism, or Lewy body disease; psychiatric disorders including depression, alcohol, or drug abuse; 2) concomitant use of psychotropic medication in large quantity; and 3) insufficient cognitive capacity to understand and cooperate with study procedures.

All patients underwent a complete physical and neurological examination, an extensive battery of neuropsychological assessments, and standard laboratory tests. Healthy volunteers underwent a brief clinical interview and MMSE to confirm that they satisfied exclusion criteria for cognitive deficits, psychoactive drug use, and clinical disorders.

All the subjects included in this study had to satisfy exclusion criteria of head movement during fMRI scanning <3 mm translation in any axis and <3° angular rotation in any axis (see data preprocessing for detail). Five participants (1 healthy volunteer, 1 patient with MCI, and 3 patients with AD) had excessive head motion during scanning, and 1 MCI patient did not have a complete set of MRI data due to technical problems during scanning. These participants were therefore excluded, leaving a sample of 21 healthy volunteers (7 males, age: 65.0 ± 8.1 years), 18 patients with MCI (10 males, age: 70.2 ± 7.9 years), and 35 patients with AD [17 mild AD (8 males, age: 66.1 ± 8.3 years) and 18 severe AD (9 males, age: 65.4 ± 8.6 years)]. Demographic and psychological characteristics of the samples are summarized in Table 1.

### *MRI Data Acquisition*

The MR images were acquired on a 3.0-T MR scanner (Magnetom Trio, Siemens, Germany). Functional MRI data were acquired using the same MR system and an echo planar imaging (EPI) sequence sensitive to blood oxygenation level-dependent (BOLD) contrast: Repetition time (TR) = 2000 ms, echo time (TE) = 30 ms, flip angle (FA) = 90°, matrix = 64 × 64, field of view (FOV) = 220 mm × 220 mm, slice thickness = 3 mm with interslice gap = 1 mm. Each brain volume comprised 32 axial slices, and each scanning session lasted for 360 s. During fMRI scanning, participants were instructed to keep their eyes closed, relax, and move as little as possible. Foam pads were used to reduce head movements and scanner noise. Sagittal $T_1$-weighted MR images were acquired by a magnetization-prepared rapid gradient-echo sequence (TR/TE = 2000/2.6 ms, FA = 9°, matrix = 256 × 224, FOV = 256 mm × 224 mm, 176 continuous sagittal slices with 1 mm thickness).

### *MRI Data Preprocessing*

#### *Functional MRI*

All the preprocessing was carried out using statistical parametric mapping (SPM8, http://www.fil.ion.ucl.ac.uk/spm). The first 10 images were discarded to allow for magnetization equilibrium; and the remaining 170 images were corrected for the acquisition time delay between different slices and then realigned to the first volume for head-motion correction. The time courses of head motion were obtained by estimating the translations in each direction and the angular rotations about each axis for each of the 170 consecutive volumes. It has recently been reported that submillimeter head motion during data scanning can have a substantial impact on some measurements of resting-state fMRI (Power et al. 2012; Satterthwaite et al. 2012; Van Dijk et al. 2012). We also evaluated group differences in head motion among the 4 groups according to the criteria of Van Dijk et al. (2012). The results showed that the 4 groups had no significant differences in head motion (1-way analysis of variances [ANOVAs] with Bonferroni-corrected post hoc $t$ tests, $P = 0.079$; Table 1). The realigned images were registered with the Montreal Neurological Institute (MNI) EPI template image using an affine transformation and resampled to 2-mm cubic voxel resolution. Several sources of spurious variance, including the estimated motion parameters, the linear drift, and the average fMRI time series in the cerebrospinal fluid (CSF) and white matter (WM) regions, were removed from the data through linear regression (Liu, Liang, et al. 2008; Zhang et al. 2012) within a brain mask generated from the MNI EPI template (Supplementary Fig. S1).

The maximal overlap discrete wavelet transform (Percival and Walden 2000) was used to decompose each individual fMRI time series into the following scales or frequency intervals: Scale 1, 0.125–0.250

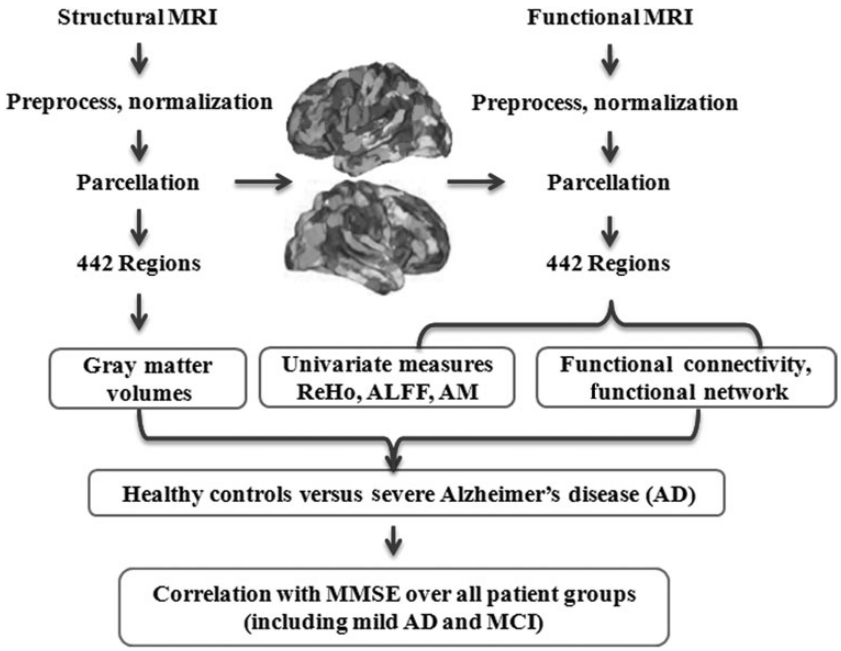


**Figure 1.** Schematic of data analysis pipeline. Regional mean fMRI time series were estimated by applying an anatomical template image to each subject's image. Univariate measures were estimated for each time series (ReHo and ALFF); bivariate measures of functional connectivity were estimated between each pair of regions; and weighted functional networks were constructed from the functional connectivity matrix for each participant. Gray matter volume was also estimated for each of the same set of 442 regions used to parcellate the fMRI data. The main statistical analyses compared the most impaired patient group, with severe AD, to the group of healthy comparison subjects on all neuroimaging markers; and correlated functional connectivity and network metrics with variation in MMSE scores over all patients (including mild AD and MCI as well as severe AD).

**Table 1**
Demographic, clinical, neuropsychological data, and head motion in NC, MCI, mild Alzheimer's disease (mAD) and severe AD (sAD)

| | NC ($n = 21$) | MCI ($n = 18$) | mAD ($n = 17$) | sAD ($n = 18$) | *P*-value |
|---|---|---|---|---|---|
| Gender (M/F) | 7/14 | 10/8 | 8/9 | 9/9 | 0.543 |
| Age (year) | 65.0 ± 8.1 | 70.2 ± 7.9 | 66.1 ± 8.3 | 65.4 ± 8.6 | 0.219 |
| Education (year) | 11.0 ± 4.4 | 9.4 ± 4.8 | 10.4 ± 4.2 | 10.9 ± 4.3 | 0.690 |
| MMSE | 28.5 ± 1.4 | 21.9 ± 5.0[a] | 14.3 ± 5.8[a,b] | 6.2 ± 4.9[a,b,c] | < 0.001 |
| CDR | 0 | 0.5 | 1.0 | 2.2 ± 0.4 | — |
| Mean head motion | 0.08 ± 0.04 | 0.10 ± 0.06 | 0.14 ± 0.13 | 0.11 ± 0.05 | 0.079 |

Note: Chi-squared test was used for gender comparisons; 1-way ANOVAs with Bonferroni-corrected post hoc *t* tests were used for age, education, and MMSE comparisons.
MMSE: mini-mental state examination; CDR: clinical dementia rating.
[a]Significant compared with NC.
[b]Significant compared with MCI.
[c]Significant compared with mild AD.

Hz; scale 2, 0.060–0.125 Hz; scale 3, 0.030–0.060 Hz; scale 4, 0.015–0.030 Hz, and scale 5, 0–0.015 Hz. Following initial analyses of functional connectivity at all scales, subsequent analysis focused on results at scale 2, which is compatible with prior studies, indicating that endogenous fMRI dynamics of neuronal origin are most salient at frequencies around 0.1 Hz (Lynall et al. 2010; Fornito et al. 2011). Finally, the wavelet-filtered images were smoothed with a 3-dimensional (3D) Gaussian kernel (6-mm full width at half maximum [FWHM]) to reduce spatial noise.

*Structural MRI*

Structural MRI data were preprocessed in SPM8 using voxel-based morphometry as implemented in the VBM8 toolbox with default parameters (http://dbm.neuro.uni-jena.de/vbm.html). Images were segmented into gray matter (GM), WM, and CSF tissue classes. The segmented images were bias corrected and registered with a template image in MNI space, using linear and nonlinear transformations (Ashburner and Friston 2005). These preliminary estimates of GM, WM, and CSF density were multiplied by the nonlinear components derived from the normalization matrix in order to preserve local information about tissue density, yielding modulated GM and WM volumes. Finally, the modulated volumes were resampled to 2-mm cubic voxel resolution and smoothed with a 3D Gaussian kernel (6-mm FWHM).

***Anatomical Parcellation***

GM areas in the brain were initially defined using FSL's cortical and subcortical Harvard-Oxford probabilistic atlas (excluding the brainstem) and the cerebellar probabilistic atlas (Diedrichsen et al. 2009) thresholded at 25%. This parcellation results in 110 anatomically-defined brain regions, which vary considerably in anatomical size (Alexander-Bloch et al. 2010). To obtain a larger number of smaller and more equally sized regional nodes, we subparcellated the GM template to define 459 regions with approximately equal size ranging from 252 to 503 voxels (2016–4024 $mm^3$; Fornito et al. 2011; Alexander-Bloch et al. 2012, 2013; for each of which we extracted mean regional time series of the preprocessed fMRI data as the represent time series. We excluded from analysis any area where there was no fMRI signal recorded from one or more participants in the study. As shown in Supplementary Figure S1 (Supplementary Material I), this resulted in a set of 442 regional areas, which subtended the whole cerebral hemispheres and did not include part of cerebellum.

***Univariate and Bivariate Measures of Spontaneous fMRI Time Series Activity***

Amplitude in the time domain (AM) and amplitude of low-frequency fluctuations (ALFF) of fMRI time series are 2 established measures of the magnitude of endogenous BOLD oscillations (Zang et al. 2007). The fMRI time series of each voxel was transformed into the frequency domain using a fast Fourier transform, and the power spectrum was estimated. The average square root of the power spectrum

was taken as the "ALFF" (Zang et al. 2007; Zuo et al. 2010):

$$\mathrm{ALFF} = \sum_{f \in \mathrm{FS}} \sqrt{\frac{|X|}{N}}, \quad (1)$$

where $X(k) = 1/N \sum_{j=1}^{N} x(j) e^{2\pi i (j1)(k1)/N}$, $f$ means the frequency. This analysis used the wavelet-filtered time series at scale 2 (0.060–0.125 Hz). AM was defined as the mean absolute value of the deviation of the BOLD signal at a voxel, $x$, from the mean value over the whole time series:

$$\mathrm{AM} = \frac{1}{N} \sum_{j=1}^{N} |x(j) \bar{X}|, \quad (2)$$

where $x(j)$ is $x$'s value at time $j$, and $\bar{X}$ is the mean of $x$ over the time series. AM is highly correlated with ALFF and, therefore, very similar results were obtained by analyzing between-group differences in terms of AM (these data are not further reported here).

Regional homogeneity (ReHo) is a measure of similarity or homogeneity of the time series in a local neighborhood of voxels (Zang et al. 2004). It is defined formally as Kendall's coefficient of concordance:

$$\mathrm{ReHo} = \frac{\sum (R_i \bar{R}_i)^2}{K^2 (n^3 n)/12} = \frac{\sum (R_i)^2 n(\bar{R})^2}{K^2 (n^3 n)/12}, \quad (3)$$

here, $R_i = \sum_{j=1}^{k} r_{ij}$is the sum rank of the $i$th time point and $r_{ij}$ is the rank of the $i$th time point of the $j$th voxel; where $\bar{R}$ is the mean of the $R_i$; over all time points $i$; $N$ is the length of the time series; and $k$ is the number of voxels within the "neighborhood" of each index voxel ($k = 27$ in the present study). ReHo ranges from 0 to 1, with the higher values indicating greater similarity of time series in the local neighborhood.

Maps of ALFF and ReHo were estimated for each voxel and standardized within each subject to generate $Z$-score maps, which could be appropriately averaged and compared across participants (Buckner et al. 2009; Zuo et al. 2010). The $Z$-score of a voxel was calculated simply by subtracting the whole map mean and dividing by the whole map standard deviation. Finally, regional estimates were calculated for each subject by averaging the $Z$-scores of the voxels in each of the 442 brain regions.

Wavelet correlation coefficients were used as bivariate measures of the functional connectivity between each pair of regional mean time series, for each individual fMRI scan. The wavelet correlation at scale 2 (corresponding to a frequency interval of 0.06–0.125 Hz) was estimated for each pair of regions, resulting in a ($442 \times 442$) wavelet correlation matrix (also known as a functional connectivity or association matrix). Fisher's $r$-to-$Z$ transformation was applied to each wavelet correlation coefficient to normalize the distribution of wavelet correlation coefficients prior to statistical testing (Liu, Liang, et al. 2008).

### *Measures of Connection Distance and Functional Network Topology*

Graphs were constructed by thresholding each subject's wavelet correlation matrix to generate binary graphs. The thresholding operation used a minimum spanning tree followed by a global connection strength cutoff (Alexander-Bloch et al. 2010), so that correlations greater than the threshold were represented as edges between the corresponding regional nodes, whereas no edges existed between regional nodes that were not more strongly correlated than the threshold. A binary graph can also be described with an adjacency matrix $A$, each element of which, $a_{ij}$, is either 1 if there is an edge between nodes $i$ and $j$, or 0 if there is not an edge between $i$ and $j$. The global connection strength cutoffs were varied for each subject so as to generate graphs at a range of connection densities, from 1% to 40% at 1% intervals, where connection density is the number of edges in the graph as a percentage of the maximum possible number of edges, $N(N-1)/2$, where $N = 442$.

The physical connection distance of an edge in the resulting graphs was simply estimated as the Euclidean distance between the centroids of the 2 functionally connected regions (Salvador, Suckling, Coleman, et al. 2005; Sepulcre et al. 2010), that is, $d_{ij} = \sqrt{(x_i - x_i)^2 + (y_i - y_i)^2 + (z_i - z_i)^2}$, where $x$, $y$, and $z$ are the coordinates of the centroid of each region in stereotactic space. These distances were normalized to the range from 0 to 1 by dividing by the longest distance in the brain, that is, $d'_{ij} = d_{ij} / \max(d_{ij})$. The global mean connection distance, $D$, was the mean distance of all the edges in a network:

$$D = \frac{1}{2m} \sum_{j \neq i, j \in G} d'_{ij}, \quad (4)$$

where $d'_{ij}$ is the normalized Euclidean distance between nodes $i$ and $j$, and $m$ is the number of edges in the graph. The nodal mean connection distance was the mean distance of all the edges of a given node.

Every edge of a graph could then be weighted by the product of the connection distance and the wavelet correlation. This defines a weighted adjacency matrix, $W$, with elements $w_{ij}$,

$$w_{ij} = d'_{ij} \times |z_{i,j}| \times a_{i,j}, \quad (5)$$

where $d'_{ij}$ is the normalized distance between nodes $i$ and $j$, $|z_{i,j}|$ is the absolute value of the $Z$-scored wavelet correlation and $a_{ij}$ is an element of the binary adjacency matrix, $A$ (Supplementary Fig. S2 for an illustration).

The clustering coefficient, $C$, is a measure of the extent of the local density or cliquishness of a network. For weighted networks, the weighted clustering coefficient of a node is defined as:

$$C_i = \frac{1}{S_i (K_i - 1)} \sum_{j,h \in G_i} \frac{w_{ij} + w_{jh}}{2} a_{ij} a_{ih} a_{jh}, \quad (6)$$

where $S_i = \sum_j w_{ij}$ denotes the strength of node $i$, $K_i$ is the binary degree of the node $i$, and $a_{ij}$ is an element of the underlying binary adjacency matrix (Barrat et al. 2004). The clustering coefficient of a network is the average of the clustering coefficients of all nodes:

$$C = \frac{1}{N} \sum_{j \in G} C_i, \quad (7)$$

where $C_i$ is the nodal clustering coefficient of node $i$, and $N$ is the number of nodes in the network.

The global efficiency, $E_{\mathrm{glob}}$, is a measure of the capacity for parallel information transfer in the network. It is defined as the inverse of the harmonic mean of the minimum path length between each pair of nodes (Latora and Marchiori 2001; Rubinov and Sporns 2010):

$$E_{\mathrm{glob}} = \frac{1}{N(N-1)} \sum_{j \neq iG} \frac{1}{L_{ij}}, \quad (8)$$

where $L_{ij}$ is the shortest path length between the $i$th node and $j$th nodes, calculated using the Dijkstra algorithm with $1/w_{ij}$ as a weight (where $w_{ij}$ is defined as in Eq. 5).

All the topological properties were estimated using in-house software (Brat, www.brainnetome.org).

### *Statistical Analysis*

We tested the null hypothesis of no difference between healthy volunteers and patients with severe AD on all measures of time series activity, connection distance, and functional network topology. We generally used a 2-sample 2-tailed $t$-test for each measure. Global network properties were tested over a wide range of connection densities (1–40%). Abnormal network properties for each patient were summarized as $Z$-scores calculated by subtracting the control group mean and dividing by the control group standard deviation (Buckner

et al. 2009; Zuo et al. 2010). For multiple comparisons between groups, for example, comparisons in terms of multiple nodal metrics of network topology we used a corrected *P*-value ($P < 1/N$) for statistical significance (Fornito et al. 2011).

In the present study, we identified significant differences in functional connectivity between healthy normal controls (NC) and patients with severe AD according to the following 2 criteria: 1) The normalized functional connectivity (*Z*-score) was significantly different from zero within each group at a highly conservative threshold of $P < 0.05$, Bonferroni corrected; 2) for the set of edges that were significantly different from zero in one or both groups, the difference in *Z*-scores between the NC and severe AD groups was tested at a conservative threshold of $P < 0.05$, false discovery rate (FDR) corrected. The second probability threshold, while retaining strong control over type 1 error in the context of multiple comparisons, is less severe than the Bonferroni correction applied to the first probability threshold, which was considered more appropriate to correct for the larger number of comparisons entailed by testing the 97 461 wavelet correlations between all possible pairs of 442 regions.

Within the brain regions defined as abnormal by comparison between the healthy volunteers and the patients with severe AD, we used Pearson's correlation coefficient to evaluate the relationship between MMSE scores and global or nodal measures of brain functional activity, functional connectivity, or functional network properties over all patients in the study, that is, including patients with MCI and mild AD as well as those with severe AD. We used the false discovery rate to control type 1 error in the context of testing correlations between MMSE scores and functional network or connectivity measures ($P < 0.05$, FDR corrected).

We also explored the correlation between MMSE scores and measures of network topology over a range of connection densities (1–10%) for global measures and at a sparse connection density (1%) for nodal measures. Because these analyses were exploratory in nature, we used a statistical significance level of $P < 0.05$ (uncorrected).

Caret v5.61 software was used to visualize the anatomical distribution of abnormal measures of functional activity, or network topology (Van Essen et al. 2001; Van Essen 2005).

## Results

### *Altered Regional fMRI Dynamics: Links to MMSE and GM Volume Changes*

We focused on 2 measures of functional MRI time series at each voxel of the images: ALFF, or ALFF, which is a measure of the strength of oscillations (Zang et al. 2007); and ReHo, which is a measure of the similarity of time series recorded from a local neighborhood of voxels (Zang et al. 2004).

The strength of resting-state fMRI oscillations measured by ALFF was significantly locally reduced in severe AD (Fig. 2). The brain regions most affected by AD included the regions of posterior cingulate cortex (PCC), precuneus (PCU), and lateral temporo-parietal cortex (middle temporal gyrus and angular gyrus) that have been previously described as components of the default mode network (Buckner et al. 2008; Laird et al. 2009). In some of these regions, between-subject variability in MMSE scores was significantly correlated with ALFF: For example, in bilateral angular gyrus, greater ALFF was associated with superior cognitive function measured by higher MMSE scores (Fig. 2 and Supplementary Fig. S3).

ReHo of oscillations was also reduced in AD; and, again, many of the regions demonstrating significant between-group differences have previously been described as components of the default mode network (Fig. 2 and Supplementary Fig. S4). In almost all regions demonstrating significant reductions of ReHo in patients with severe AD, there were intermediate degrees of abnormality in patients with mild AD or MCI (Supplementary Fig. S4). There were also significant positive correlations between ReHo and MMSE scores in many of the regions, which demonstrated significant abnormality in severe AD. This association is illustrated for the left medial occipito-parietal cortex (PCU and cuneus) in Figure 2.

Thus, there was a fair degree of overlap in the anatomical regions demonstrating abnormal fMRI dynamics measured by ALFF and ReHo. This is theoretically intuitive since greater heterogeneity of fMRI dynamics at a supravoxel or voxel neighborhood level (as measured by ReHo) might also be associated with greater heterogeneity of dynamics at a subvoxel level, which would reduce the strength of oscillations measured at a voxel level (Supplementary Fig. S3). However, although these 2 measures are theoretically and empirically correlated, ReHo seemed to be more sensitive as a marker of continuous variation in cognitive function as measured by the MMSE (Fig. 2 and Supplementary Fig. S4).

Local changes in fMRI dynamics were also related to local, disease-related changes in GM volume. As expected from prior studies, AD was associated with significant reductions of GM volume in extensive areas of cortex (Fig. 2). Greater severity of cognitive impairment (lower MMSE scores) was associated with greater loss of GM volume in regions, including PCC and bilateral temporo-parietal cortex (Fig. 2 and Supplementary Fig. S4). This is broadly compatible with a prior study (Buckner et al. 2009), suggesting that neurodegenerative changes in default mode network nodes might be of special importance in the pathogenesis of cognitive impairment and dementia.

### *Altered Inter-regional fMRI Connectivity: Links to MMSE, Regional Dynamics, and Connection Distance*

The strength of functional connectivity between fMRI time series was significantly locally reduced in patients with severe AD. Correlations between regional time series were less than normal for 370 pairs of brain regions; and these abnormal functional connections tended to be relatively long distance and were concentrated on regions including medial prefrontal and premotor cortex, PCU, and lateral temporo-parietal cortex (Fig. 3; Supplementary Figs S5 and S6). In other words, posterior default mode network regions that demonstrated abnormal local dynamics (reduced ReHo and/or ALFF) also demonstrated the reduced strength of functional connections to other brain regions, especially anatomically distant areas of medial prefrontal and premotor cortex, which have been previously described as anterior components of the default mode network (Greicius et al. 2004, 2009; Buckner et al. 2009; Laird et al. 2009). There were also a smaller number of inter-regional correlations that were significantly greater than normal in severe AD (Fig. 3). Abnormally enhanced connections were relatively short distance and concentrated on regions of the medial prefrontal cortex, which is consistent with a prior study by Wang et al. (2007).

Considering also the patients with mild AD and MCI, the strength of correlation between regional fMRI time series was significantly related to variation in MMSE scores. More severely impaired patients tended to have reduced the functional connectivity of 34 long-distance edges between anterior

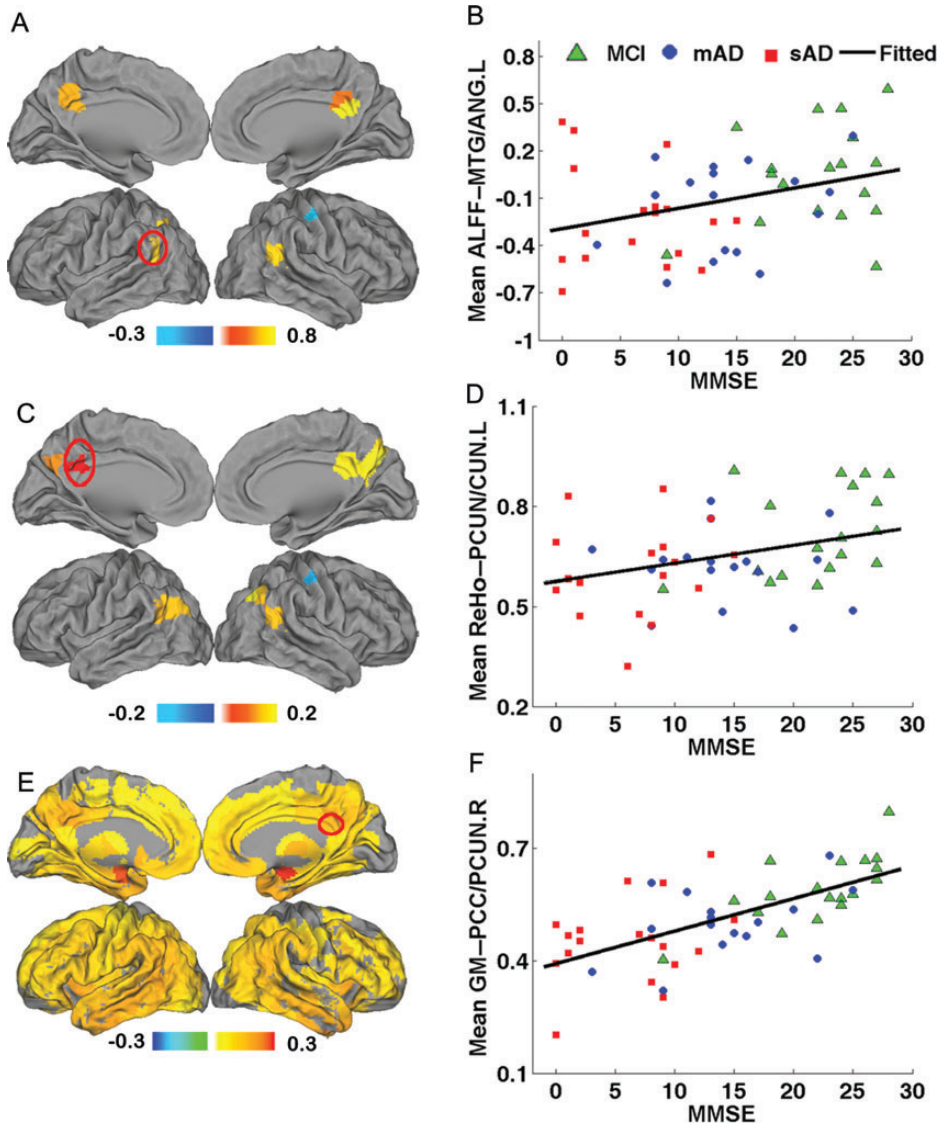


**Figure 2.** Altered univariate fMRI measures and GM density in patients with AD and MCI. (*A*) Regions showing a significant difference in ALFF between NC and patients with severe AD; red/yellow voxels indicate reduced ALFF in patients and blue voxels indicate increased ALFF in patients. (*B*) Scatterplot showing a significant association between MMSE scores for all patients and ALFF in the left temporo-parietal cortex (medial temporal gyrus and angular gyrus; $R = 0.309$, $P = 0.027$). MCI patients are indicated by green triangles, mild AD patients by blue circles, and severe AD patients by red squares. (*C*) Regions showing a significant difference in ReHo between NC and patients with severe AD; voxels are color-coded as in *A*. (*D*) Scatterplot showing the significant association between MMSE scores for all patients and ReHo in the left occipito-parietal cortex (precuneus (PCUN) and cuneus; $R = 0.361$, $P = 0.009$); diagnostic groups are distinguished by point markers as in *B*. (E) Regions showing significant GM density differences between patients with severe AD and NC; voxels are color-coded as in *A*. (*F*) Scatterplot showing the significant association between MMSE scores for all patients and GM in the left occipito-parietal cortex (PCC and PCUN; $R = 0.620$, $P < 0.0001$); diagnostic groups are distinguished by point markers as in *B*.

and posterior nodes that were abnormal in patients ($P < 0.05$, FDR corrected; Fig. 3 and Supplementary Material II).

The preferential impact of AD on long-distance functional connections was confirmed by several additional results. In both NC and patients with severe AD, the strength of functional connections between regions decreased nonlinearly as a function of increasing distance between connected regions. However, the patients with severe AD had somewhat greater strength of functional connectivity at short distances and reduced strength of connections over long distances. This effect is also evident by inspection of graphs showing the top 1% of most strongly connected pairs of regions in both the NC and patients with AD or MCI. More severe forms of disorder are associated with fewer long-distance connections (Fig. 4).

### *Altered Brain Network Architecture*

To complement these results based on analysis of the continuous measures of association between regions, we also evaluated topological properties of weighted graphs derived by thresholding individual functional connectivity matrices.

We measured global topological parameters (clustering and efficiency) and global mean connection distance for functional networks across a wide range of connection densities (1–40% of maximum possible connection density). Global efficiency was significantly reduced in patients with severe AD, and positively correlated with MMSE scores across all patient groups (Fig. 5 and Supplementary Table S3). As expected from the prior analysis on the relationship between functional connectivity and anatomical distance between connected

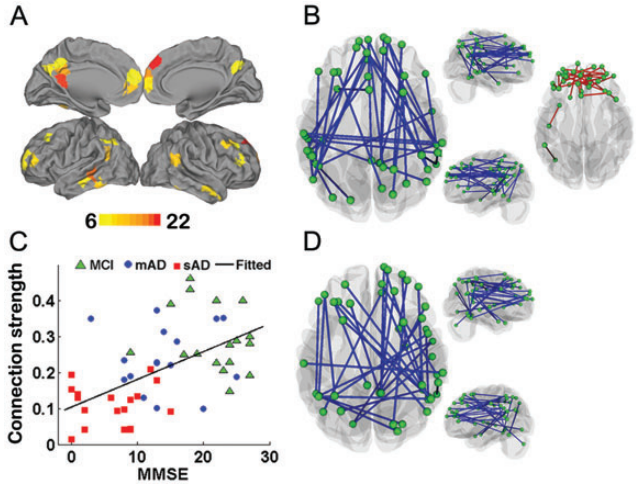


**Figure 3.** Altered functional connectivity in AD and in association with MMSE scores. (*A*) Nodal distribution of altered functional connectivities among the 442 brain regions. The color bar denotes the number of edges that had abnormally reduced the strength of connectivity to each node. (*B*) Graph showing the top 10% decreased functional and increased functional connections in patients with severe AD compared with NC ($P < 0.05$, false discovery rate (FDR) corrected). Blue line means decreased functional connectivity. Red line means increased functional connectivity. See also see Supplementary Table S1 and S2 and Figure S5 and S6 for details. (*C*) Scatterplot showing the relationship between the mean connectivity strength of the top 10% decreased functional connections and MMSE ($R = 0.523$, $P = 0.0001$). MCI patients are indicated by green triangles, mild AD patients by blue circles, and severe AD patients by red squares. (*D*) Graph showing the functional connections that are significantly correlated with MMSE in the MCI and AD groups ($P < 0.05$ FDR corrected).

regions, the global mean connection distance of functional networks was also significantly reduced in AD, and positively correlated with MMSE scores across all patient groups (Fig. 5), due to the selective attenuation of long-distance functional connections in more impaired patients. The clustering coefficient was not significantly different between groups at sparse connection densities, but was correlated with MMSE across all patient groups, including MCI and mild AD (Fig. 5 and Supplementary Fig. S7).

Topological metrics and connection distance were also estimated individually for each regional node in the networks, providing a more fine-grained resolution of disease-related effects on functional network organization. Nodal efficiency and connection distance were significantly reduced in severe AD, and positively correlated with MMSE across all patients, in the anterior and posterior components of the default mode network (Fig. 6 and Supplementary Fig. S8).

## Discussion

Here, we explored brain phenotypes associated with AD and with continuous variation in symptomatic impairment measured by the MMSE. We have combined functional and structural MRI data, using multiple complementary measures of fMRI dynamics, connectivity, and networks, to produce an internally coherent and unusually comprehensive set of results that define local and global abnormalities of brain organization in a large sample of patients expressing variable degrees of cognitive impairment.

We have found compelling evidence that functional and anatomical changes in components of the default mode network are particularly important brain markers of disease severity and cognitive impairment. Especially in the posterior default mode network components—such as PCU, lateral temporo-parietal cortex, and PCC—reduced ReHo, ALFF and GM volume were associated with lower MMSE scores. These local changes were associated with decreased strength of long-distance functional connections between anterior and posterior default mode network components (Figs 3 and 4), and decreased strength of short-distance functional connections between posterior default mode network components. Topologically, these changes in functional connectivity were paralleled by change in global and nodal properties of functional brain networks (Figs 3–6; Supplementary Figs S5 and S6). Network organization was less efficient, and associated with greater loss of long-distance connections, in patients with more severe AD. Reduced global efficiency of weighted networks was associated with a greater degree of cognitive impairment over the full range of cognitive performance represented by severe and mild AD and MCI patient groups.

The main methodological innovation of this study is that we have applied distance-weighted graph analysis to measure brain functional network organization in a large and clinically graded sample of patients with MCI, mild AD, and severe AD. To the best of our knowledge, this is the first weighted graph analysis of AD or related patient groups. As noted elsewhere, the use of weighted graphs was shown to be more sensitive to between-group differences in network organization than in unweighted graphs. It is also theoretically advantageous as a way of linking topological change, such as reduced efficiency, to changes in the spatial properties of brain networks, such as reduced connection distance. The interplay between spatial and topological properties of brain networks is central to economic models of normal brain network organization and is considered likely to be important for more complete characterization of network abnormalities in a range of brain disorders (Bullmore and Sporns 2012). The study is also novel in demonstrating an ordered progression of weighted network abnormalities across a spectrum of clinical severity, ranging from MCI to severe AD; in contextualizing the methodological innovative results by comparison with more familiar measures, for example, ReHo and functional connectivity, estimated in the same resting-state fMRI dataset; and in demonstrating that some putative fMRI biomarkers of AD are consistently abnormal in Chinese patient groups as well as in the more frequently studied Western populations of patients with MCI and AD.

### *Disrupted Long-Distance Functional Connections in AD*

Clinically, AD manifests as a combination of functional deficits: At an early stage, AD patients show functional impairments in memory, disorientation, and execution; as the disease progresses, extensive cognitive impairments, including language deterioration and memory loss, occur; and at the late stage, these patients are unable to perform even the simplest daily tasks. Considering the possibility that abnormalities of functional connectivity may exist in widely distributed brain regions in AD, it is helpful to study functional connectivity patterns for a better understanding of the pathophysiology of AD. The cognitive impairment in AD has been explained by a disturbance of the interactions between different brain areas, and the disconnection hypothesis has been

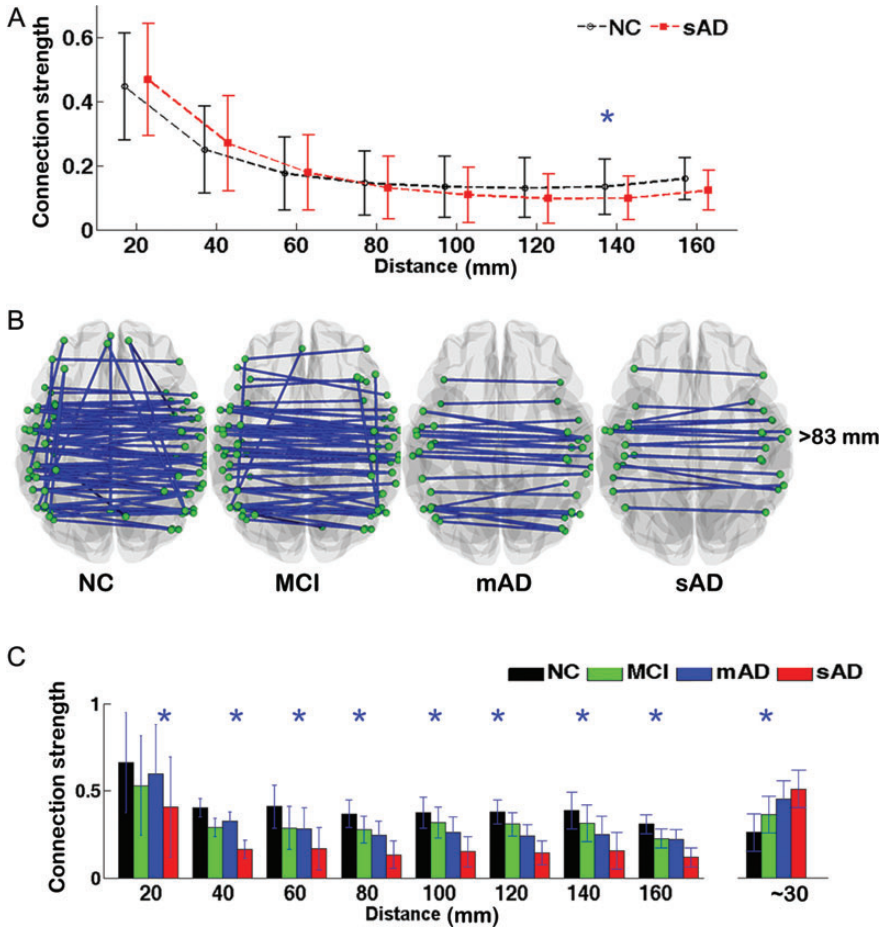


**Figure 4.** Decreased long-distance functional connectivity in AD. (*A*) Plot of the global mean connection strength at different connection distances (mm) in NC (black) and patients with severe AD (red) (error bar indicates standard deviation). Asterisk denotes a significant difference in global connection strength at $P < 0.05$. (*B*) Graph shows the functional connectivity pattern in NC, MCI, mild AD, and severe AD groups at connection density 1%. Here, we showed that the long-distance connections (> 83 mm = the mean physical distance of the brain) are significantly reduced in the patient groups, especially in severe AD. (*C*) Bar graph of connection strength at different distances for the connections that were significantly different in severe AD compared with NC: NC (black), MCI (green), mild AD (blue), and severe AD (red); error bars indicate standard deviation. Asterisk denotes a significant difference between NC and severe AD at $P < 0.05$, see Supplementary Table S1 and S2 and Figure S5 and S6 for details.

advanced in AD (Delbeuck et al. 2003, 2007; Buckner et al. 2009). Some previous studies focusing on either functional connectivity of regions of interest (such as altered functional connectivity of hippocampus, PCC, and thalamus; Wang et al. 2006; Allen et al. 2007; Wang, Liang, et al. 2011; Wang, Jia, et al. 2012), or a specific network (such as default mode network; Greicius et al. 2004; Sorg et al. 2007; Buckner et al. 2009; Neufang et al. 2011), or global functional network properties (Stam et al. 2007; Wang et al. 2007; He et al. 2008; Supekar et al. 2008; Sanz-Arigita et al. 2010), have provided convergent evidence that AD is a disconnection syndrome. Our results, for the first time, assessed brain function in AD across a wide range of univariate, bivariate, and network topological measures. We demonstrated that the impact of AD was preferentially on long-distance connections with consequential loss of global network efficiency, and that the profile of brain functional abnormalities in severe AD was generally expressed to a lesser degree in clinically less impaired patients with mild AD or MCI.

It is well known that a high level of functional interaction between different brain regions is required to support daily cognitive activities. Brain graphs are apparently simple, but powerful models of the brain connectome (Bullmore and Sporns 2009; Bullmore and Bassett 2011). The present results showed that the network topological properties were disrupted in severe AD as expected from previous fMRI (Supekar et al. 2008; Sanz-Arigita et al. 2010; Wang, Zuo, et al. 2012), structural MRI (He et al. 2008; Yao et al. 2010), EEG/MEG (Stam et al. 2006, 2007, 2009; Buldu et al. 2011), and diffusion MRI (Lo et al. 2010) studies in AD/MCI subjects. Most of these previous studies found altered network properties, such as lower efficiency or longer path length, in AD; although results are not entirely consistent across previous studies using different neuroimaging modalities (see Supplementary Table S4 for a short summary). Of note, for the first time, we introduced distance-weighted networks to model the brain architecture and found that greater degrees of cognitive impairment were associated with lower global efficiency in the patient groups (Figs 5 and 6; Supplementary Figs S7 and S8). Together with the evidence for decreased long distance, for example, anterior–posterior, functional connectivity (Figs 3 and 4; Supplementary Figs S5 and S6), our data provide strong direct support for AD as a disconnection syndrome (Delbeuck et al. 2003, 2007).

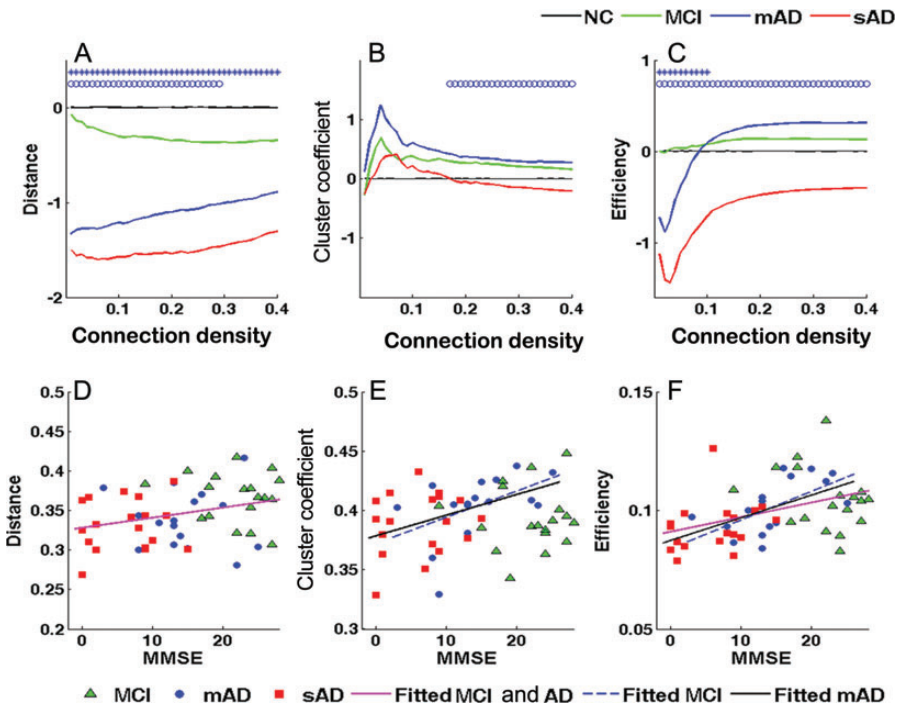


**Figure 5.** Global network topological properties were abnormal in AD and correlated with MMSE. (*A–C*) Group differences of the normalized network properties—distance (*A*), clustering (*B*), and efficiency (*C*) —over a range of connection densities from 1% to 40%. Blue stars indicate that the brain network topological properties were significantly altered in severe AD (red line) compared with NC (black line; $P < 0.05$). Blue circles indicate the brain network topological properties were significant correlated with MMSE in the MCI and AD groups ($P < 0.05$). (*D–F*) Scatterplots of the relationships between network properties—distance (*D*), clustering (*E*), and efficiency (*F*)—and MMSE in the patient groups. MCI patients are indicated by green triangles, mild AD patients by blue circles, and severe AD patients by red squares. Magenta lines indicate that brain network measures were significantly correlated with MMSE in the MCI and AD groups. Blue dashed line indicates that brain network measures were significantly correlated with MMSE in the MCI group. Black line indicates that brain network measures were significantly correlated with MMSE in the mild AD group. See Supplementary Table S3 for details.

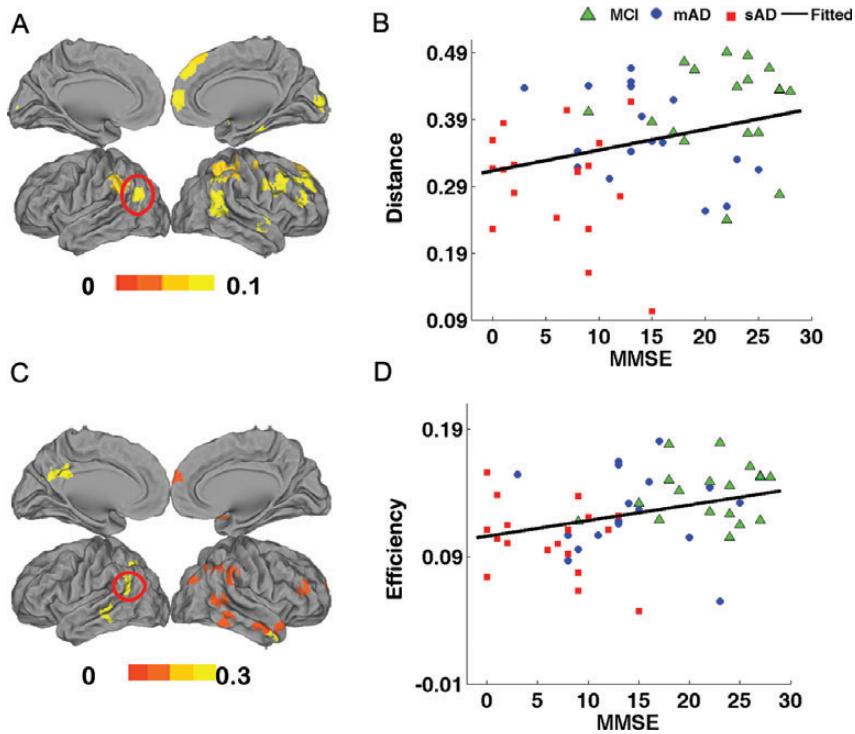


**Figure 6.** Nodal distribution of the altered topological properties in AD. (*A*) Nodal distribution of the altered distance in severe AD; red/yellow voxels indicate reduced distance in severe AD. (*B*) Scatterplot of the relationship between nodal mean distance and MMSE in the MCI and AD groups ($R = 0.389$, $P = 0.004$). MCI patients are indicated by green triangles, mild AD patients by blue circles, and severe AD patients by red squares. (*C*) Nodal distribution of the altered global efficiency in severe AD; red/yellow voxels indicate reduced global efficiency in severe AD. (*D*) Scatterplot of the relationship between nodal efficiency and MMSE in the MCI and AD groups ($R = 0.334$, $P = 0.015$). MCI patients are indicated by green triangles, mild AD patients by blue circles, and severe AD patients by red squares.

### *Impaired Cortical Hub Regions in AD*

We provided convergent evidence that the altered regions identified by both the univariate and bivariate measures largely overlapped with the classical regions of the default mode network as well as the regions of the medial temporal lobes (Figs 2 and 3). The default mode network contributes to the functions of remembering the past, envisioning future events, considering internal thoughts and perspectives, and monitoring the external environment (Raichle et al. 2001; Fox and Raichle 2007; Buckner et al. 2008). Previous results have shown that regions of the default mode network, especially the PCC and medial prefrontal cortex, are important hub regions in the human brain (Buckner et al. 2009; Sepulcre et al. 2010; Tomasi and Volkow 2010). The hub regions of the brain will exchange information with many other regions and may be expected to exert a large influence on information communication and to play a key role in facilitating functional integration between different functionally segregated brain regions (Bullmore and Sporns 2009; Sporns 2011). The preferential use of these hub regions throughout daily life might induce the increased accumulation of *Aβ*, which plays a pivotal role in the development of AD (Buckner et al. 2005; Jack et al. 2011).

It is also of note that a growing number of findings support the loss of WM integrity and/or cortical dysfunction in the default mode network in AD (Buckner et al. 2008, 2009; Liu, Wang, et al. 2008; Dickerson et al. 2009) and MCI (Sorg et al. 2007; Sperling et al. 2009; Sheline et al. 2010; Petrella et al. 2011). The continuous higher spontaneous activity and/or associated metabolism in hub regions might also explain the lesions of these hub regions in AD patients (Buckner et al. 2009). Moreover, we also noted the most affected connectivities are among the long-distance anterior–posterior connections within the default mode network (Figs 3 and 4), which confirms the altered activity pattern in these regions and is compatible with the suggested disconnection in AD (Horwitz et al. 1995; Grady et al. 2001; Delbeuck et al. 2007; Wang et al. 2007; Buckner et al. 2009; Sanz-Arigita et al. 2010).

### *The Relationship Between Brain Function and Disease Severity*

From a clinical perspective, the pathophysiological process of AD is thought to begin many years before the diagnosis of dementia (Jack et al. 2011; McKhann et al. 2011; Sperling et al. 2011). Of note, individuals with MCI are a target population for evaluating very early treatment interventions for AD since they represent not only an extension of normal aging, but also an intermediate stage between normal cognitive performance in healthy elderly people and dementia, especially AD. Many subjects with MCI harbor the pathologic changes of AD and demonstrate a higher risk for decline to AD than to healthy older individuals (Petersen et al. 1999, 2001; Petersen 2009). In accordance with the clinical features and numerous previous studies, our result also showed that there is an explicit trend of alteration in the pattern of the univariate and bivariate measures in MCI and mild AD (which were often intermediate in the value between the severe AD and healthy volunteer groups), and these measures were significantly correlated with the severity of disease (measured by MMSE). The consistency of disease-related measures across the multiple patient groups provided strong new evidence that MCI is a transitional stage of AD.

### *Limitations, Caveats, and Future Directions*

According to the principles of the brain network theoretical model, the decreased global efficiency in the AD network represents reduced capacity for information transfer in the patients. The connection strength reflects the activity coherence, while the connection distance reflects the physical distance between regions. As anticipated by prior studies (Salvador, Suckling, Coleman, et al. 2005; Salvador, Suckling, Schwarzbauer, et al. 2005), the strength of functional connectivity between regions generally decreased as a nonlinear (gravity law) function of increasing anatomical distance between regions (Alexander-Bloch et al. 2013). However, most previous graph theoretical studies did not include any measures of the physical or spatial properties of functional brain networks in AD. Recent studies have demonstrated that the human brain has short-distance and long-distance hubs (Buckner et al. 2009; Sepulcre et al. 2010). The hubs of the functional network are considered to be both cognitively important, acting as critical way stations for information processing, and metabolically expensive. Their high metabolic cost may make them more vulnerable to neurodegenerative changes and their topological importance for information processing may lead rapidly to the clinical expression of cognitive impairment as a result (Buckner et al. 2008, 2009). In keeping with the expectation that the long-distance connector hubs and connections of functional networks might be especially vulnerable to neurodegenerative processes, and critical for cognitive performance, we found strong evidence for long-distance connections to be selectively attenuated with increasing severity of AD, or increasing the degree of cognitive impairment measured by MMSE scores (Figs 3 and 4).

We consider that one of the innovative aspects of this study is the use of a distance-weighted graph analysis to demonstrate functional network abnormalities associated with variable severity of cognitive impairment. Most prior graph theoretical studies of human neuroimaging data have reduced continuous measures of structural or functional connectivity between nodes a continuous distance apart in physical space to a binary set of unweighted edges (Bullmore and Bassett 2011). The extreme simplification of unweighted graph analysis has yielded some important basic insights into the topology of human brain networks (Bullmore and Sporns 2009). But, it entails a drastic loss of information. Here, we have introduced a distance-weighted graph as a richer model of the functional network. Each edge that satisfied an arbitrary threshold for functional connectivity was weighted by the product of the Euclidean distance between the connected nodes and the strength of functional connectivity between them. The topology of this weighted graph was then quantified by weighted measures of efficiency and clustering as defined in more detail in Eqs. (7) and (8). Modeling brain networks in the same dataset by binary unweighted graphs or only strength weighted graphs substantially reduced the sensitivity of the study to demonstrate any between-group differences in network topology (Supplementary Fig. S9 versus S7). Also in another dataset, using the binary network, we only find slight difference in network properties between NC and AD patients (CDR = 2), while no significant correlations were found between network measures and MMSE (Zhao et al. 2012). Therefore, this distance-weighted analysis has proven to be sensitive to detect clinically graded

abnormalities in distance-weighted topology of human brain fMRI networks measured in patients with MCI, mild, and severe AD (Fig. 5; Supplementary Figs S7 and S9). This result suggests that, for network analysis of disorders such as AD, which impact preferentially on hub nodes mediating long-distance connections (Buckner et al. 2008, 2009; Sepulcre et al. 2010), distance-weighted graphs may provide a more diagnostically informative class of models than binary graphs. Note, however, that our estimates of physical connection distance are approximations. Future work will be needed to estimate the cortical distance with greater precision, by including information about cortical folding or WM tract length (Supekar et al. 2009; Sepulcre et al. 2010; Bozzali et al. 2011).

The MMSE is used by clinicians to help diagnose dementia and to help assess its progression and severity. However, it should be noted that MMSE is not a sensitive measure of cognition, and it will overemphasize impairments of language-related left hemisphere function and is relatively insensitive to the impairment of visuospatial-related right hemisphere function (Tombaugh and McIntyre 1992). So, the main use of the MMSE is to provide a brief clinical screening tool that quantitatively assesses the severity of cognitive impairment and documents cognitive changes occurring over time (Tombaugh and McIntyre 1992). The correlations between MMSE and connectivity/network markers indicate a general relationship between abnormal brain function and cognitive impairment that cuts across clinically categorized patient groups. The CDR was used to assign participants to the groups of MCI (CDR score = 0.5), mild AD (CDR = 1), or severe AD (CDR = 2 or 3). Thus, the CDR scores were directly related to the significant between-group differences in functional connectivity and network metrics (Supplementary Fig. S10); for example, connection distance and topological efficiency both declined as a function of increasing CDR. In future studies, it will be important to use a wider range of cognitive tests to more comprehensively assess the cognitive and behavioral variability between patients and perhaps to link specific domains of cognitive impairment to particular the measures of network organization. The analysis of cognitive phenotypes in this study is relatively broad-brush, although clinically robust.

It is important to consider the size and generalizability of this study in relation to comparable prior studies of resting-state fMRI markers in patients with AD. We identified 55 prior studies (published in recent 2 years) of resting-state fMRI markers in patients with MCI or AD. The median total sample size of the prior studies was 37 and the median size of patient groups (AD and/or MCI) was 18. Our sample comprised 74 subjects including 21 NC and 53 patients composed of 3 subgroups (Table 1). Thus, the sample size of the present study, although not large in absolute terms, was comparable with the prior literature; indeed only 2 prior studies reported larger sample sizes (Binnewijzend et al. 2012; Wang, Zuo, et al. 2012). Moreover, our sample was notable in demonstrating functional connectivity and network changes that were correlated with the severity of cognitive impairment across 3 clinically graded groups of patients, ranging from MCI through mild AD to severe AD. In terms of sample size and clinical heterogeneity, our results therefore seem likely to be generalizable. It is also relevant to note that our sample was recruited from Chinese patient populations; whereas the majority of prior studies have sampled from US or European populations. The convergence of some of our results with similar abnormalities previously reported in Western studies, for example, the consistent evidence for abnormal ReHo and functional connectivity of default mode network components, provides further support for the generalizability of the study. It also suggests that resting-state fMRI markers may potentially be sufficiently replicable to be widely useful as clinical biomarkers of AD. The sample size was sufficient to demonstrate significant between-group differences and associations with MMSE scores for multiple global and nodal metrics of brain function, even after appropriate control for the multiple comparisons entailed in testing $\sim 10^5$ pairwise functional connections between regional nodes. However, larger sample sizes in future studies might support more powerful analysis of the relationships between cognitive impairment and brain functional connectivity and network markers.

Finally, we note that it has recently been reported that sub-millimeter head motion during data scanning can have a substantial impact on some measurements of resting-state fMRI (Power et al. 2012; Satterthwaite et al. 2012; Van Dijk et al. 2012). In this context, it is notable that no subjects exceeded 3 mm of absolute rotation or translation (when compared with the first recorded time point). We also evaluated group differences in head motion among the 4 groups according to the more sensitive criteria of Van Dijk et al. (2012) and Power et al. (2012). The results showed that the 4 groups had no significant differences in mean head motion maximum head motion and framewise displacement. There was also no evidence for a significant association between MMSE scores and any measure of head motion. Hence, we consider that head motion is unlikely to provide a plausible explanation of the pattern of results we have reported.

## Supplementary Material

Supplementary material can be found at: http://www.cercor.oxfordjournals.org/.

## Funding

This work was partially supported by the National Key Basic Research and Development Program (973), grant number 2011CB707800; the Natural Science Foundation of China, grant numbers 60831004, 81270020, and 30900476; and the Natural Science Foundation of Tianjin, grant number 11JCZDJC19300. Dr Ed Bullmore is employed part time by the University of Cambridge and part time by GSK PLC and is a shareholder of G.S.K.

## Notes

The authors appreciate the suggestions of Dr Mika Rubinov from the Brain Mapping Unit, Department of Psychiatry, University of Cambridge. *Conflict of Interest*: None declared.

## References

Alexander-Bloch A, Gogtay N, Meunier D, Birn R, Clasen L, Lalonde F, Lenroot R, Giedd J, Bullmore ET. 2010. Disrupted modularity and local connectivity of brain functional networks in childhood-onset schizophrenia. Front Syst Neurosci. 4:147.

Alexander-Bloch A, Lambiotte R, Roberts B, Giedd J, Gogtay N, Bullmore E. 2012. The discovery of population differences in network

community structure: new methods and applications to brain functional networks in schizophrenia. Neuroimage. 59:3889–3900.
Alexander-Bloch A, Vertes P, Stidd R, Lalonde F, Clasen L, Rapoport J, Giedd J, Bullmore E, Gogtay N. 2013. The anatomical distance of functional connections predicts brain network topology in health and schizophrenia. Cereb cortex. 23:127–138.
Allen G, Barnard H, McColl R, Hester AL, Fields JA, Weiner MF, Ringe WK, Lipton AM, Brooker M, McDonald E et al. 2007. Reduced hippocampal functional connectivity in Alzheimer disease. Arch Neurol. 64:1482–1487.
American Psychiatric Association. 1994. Diagnostic and statistical manual of mental disorders: DSM-IV. 4th ed. Washington (DC): American Psychiatric Association.
Ashburner J, Friston KJ. 2005. Unified segmentation. Neuroimage. 26:839–851.
Bai F, Watson DR, Yu H, Shi Y, Yuan Y, Zhang Z. 2009. Abnormal resting-state functional connectivity of posterior cingulate cortex in amnestic type mild cognitive impairment. Brain Res. 1302:167–174.
Bajo R, Maestu F, Nevado A, Sancho M, Gutierrez R, Campo P, Castellanos NP, Gil P, Moratti S, Pereda E et al. 2010. Functional connectivity in mild cognitive impairment during a memory task: implications for the disconnection hypothesis. J Alzheimers Dis. 22:183–193.
Barrat A, Barthelemy M, Pastor-Satorras R, Vespignani A. 2004. The architecture of complex weighted networks. Proc Natl Acad Sci USA. 101:3747–3752.
Binnewijzend MA, Schoonheim MM, Sanz-Arigita E, Wink AM, van der Flier WM, Tolboom N, Adriaanse SM, Damoiseaux JS, Scheltens P, van Berckel BN et al. 2012. Resting-state fMRI changes in Alzheimer's disease and mild cognitive impairment. Neurobiol Aging. 33:2018–2028.
Bozzali M, Parker GJ, Serra L, Embleton K, Gili T, Perri R, Caltagirone C, Cercignani M. 2011. Anatomical connectivity mapping: a new tool to assess brain disconnection in Alzheimer's disease. Neuroimage. 54:2045–2051.
Buckner RL, Andrews-Hanna JR, Schacter DL. 2008. The brain's default network: anatomy, function, and relevance to disease. Ann N Y Acad Sci. 1124:1–38.
Buckner RL, Sepulcre J, Talukdar T, Krienen FM, Liu H, Hedden T, Andrews-Hanna JR, Sperling RA, Johnson KA. 2009. Cortical hubs revealed by intrinsic functional connectivity: mapping, assessment of stability, and relation to Alzheimer's disease. J Neurosci. 29:1860–1873.
Buckner RL, Snyder AZ, Shannon BJ, LaRossa G, Sachs R, Fotenos AF, Sheline YI, Klunk WE, Mathis CA, Morris JC et al. 2005. Molecular, structural, and functional characterization of Alzheimer's disease: evidence for a relationship between default activity, amyloid, and memory. J Neurosci. 25:7709–7717.
Buldu JM, Bajo R, Maestu F, Castellanos N, Leyva I, Gil P, Sendina-Nadal I, Almendral JA, Nevado A, del-Pozo F et al. 2011. Reorganization of functional networks in mild cognitive impairment. PLoS One. 6:e19584.
Bullmore E, Bassett D. 2011. Brain graphs: graphical models of the human brain connectome. Annu Rev Clin Psychol. 7:113–140.
Bullmore E, Sporns O. 2009. Complex brain networks: graph theoretical analysis of structural and functional systems. Nat Rev Neurosci. 10:186–198.
Bullmore E, Sporns O. 2012. The economy of brain network organization. Nat Rev Neurosci. 13:336–349.
Celone KA, Calhoun VD, Dickerson BC, Atri A, Chua EF, Miller SL, DePeau K, Rentz DM, Selkoe DJ, Blacker D et al. 2006. Alterations in memory networks in mild cognitive impairment and Alzheimer's disease: an independent component analysis. J Neurosci. 26:10222–10231.
Choo IH, Lee DY, Youn JC, Jhoo JH, Kim KW, Lee DS, Lee JS, Woo JI. 2007. Topographic patterns of brain functional impairment progression according to clinical severity staging in 116 Alzheimer disease patients: FDG-PET study. Alzheimer Dis Assoc Disord. 21:77–84.
Delbeuck X, Collette F, Van der Linden M. 2007. Is Alzheimer's disease a disconnection syndrome? Evidence from a crossmodal audio-visual illusory experiment. Neuropsychologia. 45:3315–3323.
Delbeuck X, Van der Linden M, Collette F. 2003. Alzheimer's disease as a disconnection syndrome? Neuropsychol Rev. 13:79–92.
Dickerson BC, Bakkour A, Salat DH, Feczko E, Pacheco J, Greve DN, Grodstein F, Wright CI, Blacker D, Rosas HD et al. 2009. The cortical signature of Alzheimer's disease: regionally specific cortical thinning relates to symptom severity in very mild to mild AD dementia and is detectable in asymptomatic amyloid-positive individuals. Cereb Cortex. 19:497–510.
Diedrichsen J, Balsters JH, Flavell J, Cussans E, Ramnani N. 2009. A probabilistic MR atlas of the human cerebellum. Neuroimage. 46:39–46.
Fischer P, Jungwirth S, Zehetmayer S, Weissgram S, Hoenigschnabl S, Gelpi E, Krampla W, Tragl KH. 2007. Conversion from subtypes of mild cognitive impairment to Alzheimer dementia. Neurology. 68:288–291.
Fornito A, Zalesky A, Bassett DS, Meunier D, Ellison-Wright I, Yucel M, Wood SJ, Shaw K, O'Connor J, Nertney D et al. 2011. Genetic influences on cost-efficient organization of human cortical functional networks. J Neurosci. 31:3261–3270.
Fox MD, Raichle ME. 2007. Spontaneous fluctuations in brain activity observed with functional magnetic resonance imaging. Nat Rev Neurosci. 8:700–711.
Grady CL, Furey ML, Pietrini P, Horwitz B, Rapoport SI. 2001. Altered brain functional connectivity and impaired short-term memory in Alzheimer's disease. Brain. 124:739–756.
Greicius MD, Srivastava G, Reiss AL, Menon V. 2004. Default-mode network activity distinguishes Alzheimer's disease from healthy aging: evidence from functional MRI. Proc Natl Acad Sci USA. 101:4637–4642.
Greicius MD, Supekar K, Menon V, Dougherty RF. 2009. Resting-state functional connectivity reflects structural connectivity in the default mode network. Cereb Cortex. 19:72–78.
He Y, Chen Z, Evans A. 2008. Structural insights into aberrant topological patterns of large-scale cortical networks in Alzheimer's disease. J Neurosci. 28:4756–4766.
He Y, Wang L, Zang Y, Tian L, Zhang X, Li K, Jiang T. 2007. Regional coherence changes in the early stages of Alzheimer's disease: a combined structural and resting-state functional MRI study. Neuroimage. 35:488–500.
Horwitz B. 2003. The elusive concept of brain connectivity. Neuroimage. 19:466–470.
Horwitz B, McIntosh AR, Haxby JV, Furey M, Salerno JA, Schapiro MB, Rapoport SI, Grady CL. 1995. Network analysis of PET-mapped visual pathways in Alzheimer type dementia. Neuroreport. 6:2287–2292.
Jack CR Jr, Albert MS, Knopman DS, McKhann GM, Sperling RA, Carrillo MC, Thies B, Phelps CH. 2011. Introduction to the recommendations from the National Institute on Aging-Alzheimer's Association workgroups on diagnostic guidelines for Alzheimer's disease. Alzheimers Dement. 7:257–262.
Laird AR, Eickhoff SB, Li K, Robin DA, Glahn DC, Fox PT. 2009. Investigating the functional heterogeneity of the default mode network using coordinate-based meta-analytic modeling. J Neurosci. 29:14496–14505.
Landau SM, Harvey D, Madison CM, Reiman EM, Foster NL, Aisen PS, Petersen RC, Shaw LM, Trojanowski JQ, Jack CR Jr et al. 2010. Comparing predictors of conversion and decline in mild cognitive impairment. Neurology. 75:230–238.
Latora V, Marchiori M. 2001. Efficient behavior of small-world networks. Phys Rev Lett. 87:198701.
Li SJ, Li Z, Wu G, Zhang MJ, Franczak M, Antuono PG. 2002. Alzheimer Disease: evaluation of a functional MR imaging index as a marker. Radiology. 225:253–259.
Liu Y, Liang M, Zhou Y, He Y, Hao Y, Song M, Yu C, Liu H, Liu Z, Jiang T. 2008. Disrupted small-world networks in schizophrenia. Brain. 131:945–961.
Liu Y, Wang K, Yu C, He Y, Zhou Y, Liang M, Wang L, Jiang T. 2008. Regional homogeneity, functional connectivity and imaging

markers of Alzheimer's disease: a review of resting-state fMRI studies. Neuropsychologia. 46:1648–1656.
Lo CY, Wang PN, Chou KH, Wang J, He Y, Lin CP. 2010. Diffusion tensor tractography reveals abnormal topological organization in structural cortical networks in Alzheimer's disease. J Neurosci. 30:16876–16885.
Lustig C, Snyder AZ, Bhakta M, O'Brien KC, McAvoy M, Raichle ME, Morris JC, Buckner RL. 2003. Functional deactivations: change with age and dementia of the Alzheimer type. Proc Natl Acad Sci USA. 100:14504–14509.
Lynall ME, Bassett DS, Kerwin R, McKenna PJ, Kitzbichler M, Muller U, Bullmore E. 2010. Functional connectivity and brain networks in schizophrenia. J Neurosci. 30:9477–9487.
Maioli F, Coveri M, Pagni P, Chiandetti C, Marchetti C, Ciarrocchi R, Ruggero C, Nativio V, Onesti A, D'Anastasio C et al. 2007. Conversion of mild cognitive impairment to dementia in elderly subjects: a preliminary study in a memory and cognitive disorder unit. Arch Gerontol Geriatr. 44(Suppl 1):233–241.
McKhann G, Drachman D, Folstein M, Katzman R, Price D, Stadlan EM. 1984. Clinical diagnosis of Alzheimer's disease: report of the NINCDS-ADRDA Work Group under the auspices of Department of Health and Human Services Task Force on Alzheimer's Disease. Neurology. 34:939–944.
McKhann GM, Knopman DS, Chertkow H, Hyman BT, Jack CR Jr, Kawas CH, Klunk WE, Koroshetz WJ, Manly JJ, Mayeux R et al. 2011. The diagnosis of dementia due to Alzheimer's disease: recommendations from the National Institute on Aging-Alzheimer's Association workgroups on diagnostic guidelines for Alzheimer's disease. Alzheimers Dement. 7:263–269.
Morris JC. 1993. The Clinical Dementia Rating (CDR): current version and scoring rules. Neurology. 43:2412–2414.
Neufang S, Akhrif A, Riedl V, Forstl H, Kurz A, Zimmer C, Sorg C, Wohlschlager AM. 2011. Disconnection of frontal and parietal areas contributes to impaired attention in very early Alzheimer's disease. J Alzheimers Dis. 25:309–321.
Pariente J, Cole S, Henson R, Clare L, Kennedy A, Rossor M, Cipoloti L, Puel M, Demonet JF, Chollet F et al. 2005. Alzheimer's patients engage an alternative network during a memory task. Ann Neurol. 58:870–879.
Percival D, Walden A. 2000. Wavelet methods for time series analysis. Cambridge (UK): Cambridge UP.
Petersen RC. 2009. Early diagnosis of Alzheimer's disease: is MCI too late? Curr Alzheimer Res. 6:324–330.
Petersen RC, Doody R, Kurz A, Mohs RC, Morris JC, Rabins PV, Ritchie K, Rossor M, Thal L, Winblad B. 2001. Current concepts in mild cognitive impairment. Arch Neurol. 58:1985–1992.
Petersen RC, Smith GE, Waring SC, Ivnik RJ, Tangalos EG, Kokmen E. 1999. Mild cognitive impairment: clinical characterization and outcome. Arch Neurol. 56:303–308.
Petrella JR, Sheldon FC, Prince SE, Calhoun VD, Doraiswamy PM. 2011. Default mode network connectivity in stable vs progressive mild cognitive impairment. Neurology. 76:511–517.
Power JD, Barnes KA, Snyder AZ, Schlaggar BL, Petersen SE. 2012. Spurious but systematic correlations in functional connectivity MRI networks arise from subject motion. Neuroimage. 59:2142–2154.
Pozueta A, Rodriguez-Rodriguez E, Vazquez-Higuera JL, Mateo I, Sanchez-Juan P, Gonzalez-Perez S, Berciano J, Combarros O. 2011. Detection of early Alzheimer's disease in MCI patients by the combination of MMSE and an episodic memory test. BMC Neurol. 11:78.
Raichle ME, MacLeod AM, Snyder AZ, Powers WJ, Gusnard DA, Shulman GL. 2001. A default mode of brain function. Proc Natl Acad Sci USA. 98:676–682.
Rami L, Gomez-Anson B, Sanchez-Valle R, Bosch B, Monte GC, Llado A, Molinuevo JL. 2007. Longitudinal study of amnesic patients at high risk for Alzheimer's disease: clinical, neuropsychological and magnetic resonance spectroscopy features. Dement Geriatr Cogn Disord. 24:402–410.
Rombouts SA, Barkhof F, Goekoop R, Stam CJ, Scheltens P. 2005. Altered resting state networks in mild cognitive impairment and mild Alzheimer's disease: an fMRI study. Hum Brain Mapp. 26:231–239.
Rombouts SA, Goekoop R, Stam CJ, Barkhof F, Scheltens P. 2005. Delayed rather than decreased BOLD response as a marker for early Alzheimer's disease. Neuroimage. 26:1078–1085.
Rubinov M, Sporns O. 2010. Complex network measures of brain connectivity: uses and interpretations. Neuroimage. 52:1059–1069.
Salvador R, Suckling J, Coleman MR, Pickard JD, Menon D, Bullmore E. 2005. Neurophysiological architecture of functional magnetic resonance images of human brain. Cereb Cortex. 15:1332–1342.
Salvador R, Suckling J, Schwarzbauer C, Bullmore E. 2005. Undirected graphs of frequency-dependent functional connectivity in whole brain networks. Philos Trans R Soc Lond B Biol Sci. 360:937–946.
Sanz-Arigita EJ, Schoonheim MM, Damoiseaux JS, Rombouts SA, Maris E, Barkhof F, Scheltens P, Stam CJ. 2010. Loss of 'small-world' networks in Alzheimer's disease: graph analysis of fMRI resting-state functional connectivity. PLoS One. 5:e13788.
Satterthwaite TD, Wolf DH, Loughead J, Ruparel K, Elliott MA, Hakonarson H, Gur RC, Gur RE. 2012. Impact of in-scanner head motion on multiple measures of functional connectivity: relevance for studies of neurodevelopment in youth. Neuroimage. 60:623–632.
Sepulcre J, Liu H, Talukdar T, Martincorena I, Yeo BT, Buckner RL. 2010. The organization of local and distant functional connectivity in the human brain. PLoS Comput Biol. 6:e1000808.
Sheline YI, Raichle ME, Snyder AZ, Morris JC, Head D, Wang S, Mintun MA. 2010. Amyloid plaques disrupt resting state default mode network connectivity in cognitively normal elderly. Biol Psychiatry. 67:584–587.
Sorg C, Riedl V, Muhlau M, Calhoun VD, Eichele T, Laer L, Drzezga A, Forstl H, Kurz A, Zimmer C et al. 2007. Selective changes of resting-state networks in individuals at risk for Alzheimer's disease. Proc Natl Acad Sci USA. 104:18760–18765.
Sperling RA, Aisen PS, Beckett LA, Bennett DA, Craft S, Fagan AM, Iwatsubo T, Jack CR Jr, Kaye J, Montine TJ et al. 2011. Toward defining the preclinical stages of Alzheimer's disease: recommendations from the National Institute on Aging-Alzheimer's Association workgroups on diagnostic guidelines for Alzheimer's disease. Alzheimers Dement. 7:280–292.
Sperling RA, Laviolette PS, O'Keefe K, O'Brien J, Rentz DM, Pihlajamaki M, Marshall G, Hyman BT, Selkoe DJ, Hedden T et al. 2009. Amyloid deposition is associated with impaired default network function in older persons without dementia. Neuron. 63:178–188.
Sporns O. 2011. The human connectome: a complex network. Ann N Y Acad Sci. 1224:109–125.
Sporns O. 2010. Networks of the brain. Cambridge (MA): The MIT Press.
Sporns O, Zwi JD. 2004. The small world of the cerebral cortex. Neuroinformatics. 2:145–162.
Stam CJ, de Haan W, Daffertshofer A, Jones BF, Manshanden I, van Cappellen van Walsum AM, Montez T, Verbunt JP, de Munck JC, van Dijk BW et al. 2009. Graph theoretical analysis of magnetoencephalographic functional connectivity in Alzheimer's disease. Brain. 132:213–224.
Stam CJ, Jones BF, Manshanden I, van Cappellen van Walsum AM, Montez T, Verbunt JP, de Munck JC, van Dijk BW, Berendse HW, Scheltens P. 2006. Magnetoencephalographic evaluation of resting-state functional connectivity in Alzheimer's disease. Neuroimage. 32:1335–1344.
Stam CJ, Jones BF, Nolte G, Breakspear M, Scheltens P. 2007. Small-world networks and functional connectivity in Alzheimer's disease. Cereb Cortex. 17:92–99.
Supekar K, Menon V, Rubin D, Musen M, Greicius MD. 2008. Network analysis of intrinsic functional brain connectivity in Alzheimer's disease. PLoS Comput Biol. 4:e1000100.
Supekar K, Musen M, Menon V. 2009. Development of large-scale functional brain networks in children. PLoS Biol. 7:e1000157.
Tomasi D, Volkow ND. 2010. Functional connectivity density mapping. Proc Natl Acad Sci USA. 107:9885–9890.
Tombaugh TN, McIntyre NJ. 1992. The mini-mental state examination: a comprehensive review. J Am Geriatr Soc. 40:922–935.

Tononi G, Edelman GM, Sporns O. 1998. Complexity and coherency: integrating information in the brain. Trends Cogn Sci. 2:474–484.
Van Dijk KR, Sabuncu MR, Buckner RL. 2012. The influence of head motion on intrinsic functional connectivity MRI. Neuroimage. 59:431–438.
Van Essen DC. 2005. A Population-Average, Landmark- and Surface-based (PALS) atlas of human cerebral cortex. Neuroimage. 28:635–662.
Van Essen DC, Drury HA, Dickson J, Harwell J, Hanlon D, Anderson CH. 2001. An integrated software suite for surface-based analyses of cerebral cortex. J Am Med Inform Assoc. 8:443–459.
Wang J, Zuo X, Dai Z, Xia M, Zhao Z, Zhao X, Jia J, Han Y, He Y. 2012. Disrupted functional brain connectome in individuals at risk for Alzheimer's disease. Biol Psychiatry (in press).
Wang K, Liang M, Wang L, Tian L, Zhang X, Li K, Jiang T. 2007. Altered functional connectivity in early Alzheimer's disease: a resting-state fMRI study. Hum Brain Mapp. 28:967–978.
Wang L, Zang Y, He Y, Liang M, Zhang X, Tian L, Wu T, Jiang T, Li K. 2006. Changes in hippocampal connectivity in the early stages of Alzheimer's disease: evidence from resting state fMRI. Neuroimage. 31:496–504.
Wang Z, Jia X, Liang P, Qi Z, Yang Y, Zhou W, Li K. 2012. Changes in thalamus connectivity in mild cognitive impairment: evidence from resting state fMRI. Eur J Radiol. 81:277–285.
Wang Z, Liang P, Jia X, Qi Z, Yu L, Yang Y, Zhou W, Lu J, Li K. 2011. Baseline and longitudinal patterns of hippocampal connectivity in mild cognitive impairment: evidence from resting state fMRI. J Neurol Sci. 309:79–85.
Wang Z, Yan C, Zhao C, Qi Z, Zhou W, Lu J, He Y, Li K. 2011. Spatial patterns of intrinsic brain activity in mild cognitive impairment and Alzheimer's disease: a resting-state functional MRI study. Hum Brain Mapp. 32:1720–1740.
Yao Z, Zhang Y, Lin L, Zhou Y, Xu C, Jiang T. 2010. Abnormal cortical networks in mild cognitive impairment and Alzheimer's disease. PLoS Comput Biol. 6:e1001006.
Zang Y, He Y, Zhu C, Cao Q, Sui M, Liang M, Tian L, Jiang T, Wang Y. 2007. Altered baseline brain activity in children with ADHD revealed by resting-state functional MRI. Brain Dev. 29:83–91.
Zang Y, Jiang T, Lu Y, He Y, Tian L. 2004. Regional homogeneity approach to fMRI data analysis. Neuroimage. 22:394–400.
Zhang Z, Liu Y, Jiang T, Zhou B, An N, Dai H, Wang P, Niu Y, Wang L, Zhang X. 2012. Altered spontaneous activity in Alzheimer's disease and mild cognitive impairment revealed by regional homogeneity. Neuroimage. 59:1429–1440.
Zhao X, Liu Y, Wang X, Liu B, Xi Q, Guo Q, Jiang H, Jiang T, Wang P. 2012. Disrupted small-world brain networks in moderate Alzheimer's disease: a resting-state FMRI study. PLoS One. 7: e33540.
Zuo XN, Di Martino A, Kelly C, Shehzad ZE, Gee DG, Klein DF, Castellanos FX, Biswal BB, Milham MP. 2010. The oscillating brain: complex and reliable. Neuroimage. 49:1432–1445.